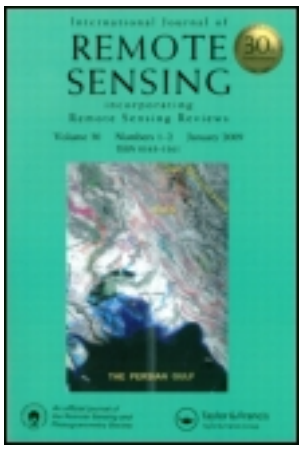


International Journal of Remote Sensing

Publication details, including instructions for authors and subscription information:
http://www.tandfonline.com/loi/tres20

# Spectral discrimination of Phytophthora infestans infection on tomatoes based on principal component and cluster analyses

M. Zhang, X. Liu & M. O'Neill

Available online: 25 Nov 2010

To cite this article: M. Zhang, X. Liu & M. O'Neill (2002): Spectral discrimination of Phytophthora infestans infection on tomatoes based on principal component and cluster analyses, International Journal of Remote Sensing, 23:6, 1095-1107

To link to this article: http://dx.doi.org/10.1080/01431160110106078

INT. J. REMOTE SENSING, 2002, VOL. 23, NO. 6, 1095–1107



# Spectral discrimination of *Phytophthora infestans* infection on tomatoes based on principal component and cluster analyses

M. ZHANG, X. LIU and M. O'NEILL

Department of Land, Air and Water Resources, University of California, Davis, California 95616, USA; e-mail: mhzhang@ucdavis.edu

(*Received 5 September 2000; in final form 18 June 2001*)

**Abstract.** Statistical methods like principal component analysis and cluster analysis are not new in identification and classification for biological features. However, the success of utilizing these two methods in discriminating late blight infected tomatoes (caused by *Phytophthora infestans*) from healthy ones has not yet been reported. This paper demonstrates the capability of using principal component analysis and cluster analysis for identification and discrimination of spectral characteristics of late blight infections on tomatoes. Our results show that the first principal component is related to the spectral properties of healthy tomatoes, and the second principal component is related to the spectral properties of infected tomatoes. Cluster analysis shows that a reasonable discrimination is obtained when the centroid distance of clusters is above 0.5. The consistent results from both principal components analysis and cluster analysis indicate that late blight infection on tomatoes can be successfully detected with remote sensing when the infection severity reaches middle to late stages. Moreover, spectral ratio analysis provides us with the way to identify the sensitive spectral wavelengths where distinguishable reflectance values can be observed for unique biological features. Understanding the light responses to unique biological features may increase discrimination accuracy by reducing the impact of soil background on spectral measurements, and utilizing the most sensitive wavelengths for discriminating between healthy and diseased tomatoes.



## 1. Introduction

Detecting plant health conditions is of primary importance to agricultural field management (Bryant and Moran 1999). It is common that the health conditions of a crop are assessed by direct methods such as scouting and checking plant canopies in the field. However, this method is time and labour intensive and usually results in a cost increase for disease monitoring in large-scale farming. It is also possible that diseased crops examined by human eyes are only detected at the later stages of infection, which is too late to employ proper disease control measures to recover crop productivity.

With the advancing airplane and satellite technologies there has been a growing interest in using optical remote sensors for mapping and monitoring crop diseases in real-time at the local scale (Bryant and Moran 1999, Deguise *et al.* 1998). Several studies have demonstrated the possibility of using remote sensing to discriminate between healthy plants, and unhealthy or diseased plants (Lillesand and Kiefer 1994, Holden and LeDrew 1998, Holden *et al.* 1999, Leblanc *et al.* 1999). In these applications, the ability to differentiate spectra of different materials is essential (Bowman

*International Journal of Remote Sensing*
ISSN 0143-1161 print/ISSN 1366-5901 online © 2002 Taylor & Francis Ltd
http://www.tandf.co.uk/journals
DOI: 10.1080/01431160110106078

*et al.* 1999, Deguise and Staenz 1999, Winter and Schlangen 1999). Perhaps even more difficult is the ability to discriminate spectra of different infection stages.

Late blight is an aggressive plant disease caused by the fungus *Phytophthora infestans*. Symptoms of late blight first appear on the leaves as water-soaked areas that rapidly enlarge to form purple-brown, oily blotches. On the lower side of the leaves, rings of grayish white mycelium and spore-forming structures may appear around the blotches. Entire leaves die and infections quickly spread to petioles and young stems. Infected fruit turn brown but remain firm unless infected by secondary decay organisms. These symptoms usually begin on the shoulders of the fruit because spores land on the fruit from above. Late blight is found when humid conditions coincide with mild temperatures for prolonged periods. Most rapid development occurs when humidity is above 90% and the average temperature is in the range of 16°C to 26°C. Losses can be severe if weather and field conditions are ideal for disease development and wind can spread the spores to other plants.

Our hypothesis was that plants in different infection stages have distinct spectral reflectance responses based on the presence (in different magnitudes) or absence of chlorophyll, and water content contained in plant leaves. Using spectra of tomato plants infected with late blight, we combined the spectral characteristics of chlorophyll and water in visible and near infrared wavelengths to test this hypothesis for possible application of remote sensing in tomato disease detection.

The objective of the study was to investigate the feasibility of using satellite or airborne passive high spectral resolution radiometers to detect plant stresses caused by late blight infection in visible and near infrared (NIR) wavelengths. We expect the results of the study can be utilized to gain an understanding of light responses to infected plants, and to classify images for disease management in precision farming.

## 2. Materials and Methods

### 2.1. *Data collection*

We collected spectral data in four fields (South Central Murphy, Meyer 119, Doud 15, and Meyer 206) near King City in the Salinas Valley, California. These field spectra were collected at about 1m above the tomato canopies that had various infection stages of late blight under actual field conditions. The spectroradiometer-GER2600 with a single field-of-view of 23 degrees was used for the data collection. This instrument was configured to acquire spectra over the 350–2500 nm range with a spectral sampling interval of 2 nm. In addition to collecting spectra of the canopies with various infection stages, we also collected soil spectra at each field.

We rated late blight infection severity into five stages (table 1): stage 1—one lesion on one or two canopy leaves, stage 2—one lesion on more than two canopy leaves, stage 3—two lesions on one to many canopy leaves, stage 4—two lesions on

Table 1. Late blight infection stages and symptoms.

| Infection stages | Symptoms |
|---|---|
| LB1 | One lesion on one or two canopy leaves |
| LB2 | One lesion on more than two canopy leaves |
| LB3 | Two lesions on one to many canopy leaves |
| LB4 | Two lesions on over half the canopy leaves |
| LB5 | Lesions dominate canopy leaves |

over half the canopy leaves, stage 5—lesions dominate the canopy leaves. Accordingly stage 1 represents the light infection and stage 5 the severe one.

### 2.2. *Data analysis*

#### 2.2.1. *Data organization*

After examining the spectral data, we found that we had collected more spectra of healthy tomato canopies than the spectra of tomato canopies with infection stages 3 and 4. In order to minimize the possible statistical impact of the uneven numbers of spectra within each field on the analysis results, we generated a new data set by combining data from all four fields. Some of the original spectra looked abnormal and may well not represent the infected canopy conditions. Hence, we applied the following two rules to clean the spectra before further analysis. First, spectra from one type of vegetation should only contain random errors so that all spectra curves for this type of vegetation uniformly concentrate in a limited curve buffer within two standard deviations. If a spectrum was outside this buffer, it was considered abnormal, and was removed from the data pool. Second, spectra from one type of vegetation should all have a similar shape or curve structure. If a spectrum had a different shape or curve structure, we again removed it from the data set for further analysis.

Using these two rules, we interactively preprocessed the collected data and obtained a new data set with 66 spectral samples. Among these 66 spectra, 22 were for healthy tomato plants (figure 1(a)), 11 for late blight infection stage 1 (figure 1(b)), 12 for stage 2 (figure 1(c)), 17 for stage 3 (figure 1(d)), and 4 for stage 4 (figure 1(e)). No spectra were obtained for stage 5. The sample size for each stage was big enough for conducting a statistical analysis even though they were not equal. This guaranteed that the analysis results would not be significantly impacted by the unequal sample size of each stage.

Comparison of soil spectra indicated that there was little difference from location to location. Almost no differences between the wavelengths of 400–680 nm were observed among the collected soil spectra. The largest soil reflectance difference was only 0.06% of the reflectance values found in the wavelengths of 750–1000 nm. Therefore, we could reasonably assume that the influence of the soils in these locations was minimal. Moreover, the exposure of soils in the canopy at the time of spectra collection was also minimal. These two features justified the removal of soil spectra from the principal component analysis.

#### 2.2.2. *Principal component analysis*

Principal component analysis (PCA) has been effectively used in many studies as a data reduction technique (Dunteman 1984). Since the method preserves the total variance while minimizing the mean square approximate errors, it is also often used as a means of identifying the data with dominant features (Fung and LeDrew 1987). The basic function of PCA is to transform the original data set into a substantially smaller and easier to interpret set of uncorrelated variables that represent most of the information in the original data set (Dunteman 1984). After PCA, the principal components can be derived from the original data set. The first component accounts for the maximum proportion of the variance in the original data set, and the subsequent orthogonal components account for the maximum remaining variance and so forth (Fung and LeDrew 1987). We used PCA to reduce the spectral samples to represent/investigate the association of the spectral properties of healthy tomato plants and infected tomato plants. Taking each spectrum as a random

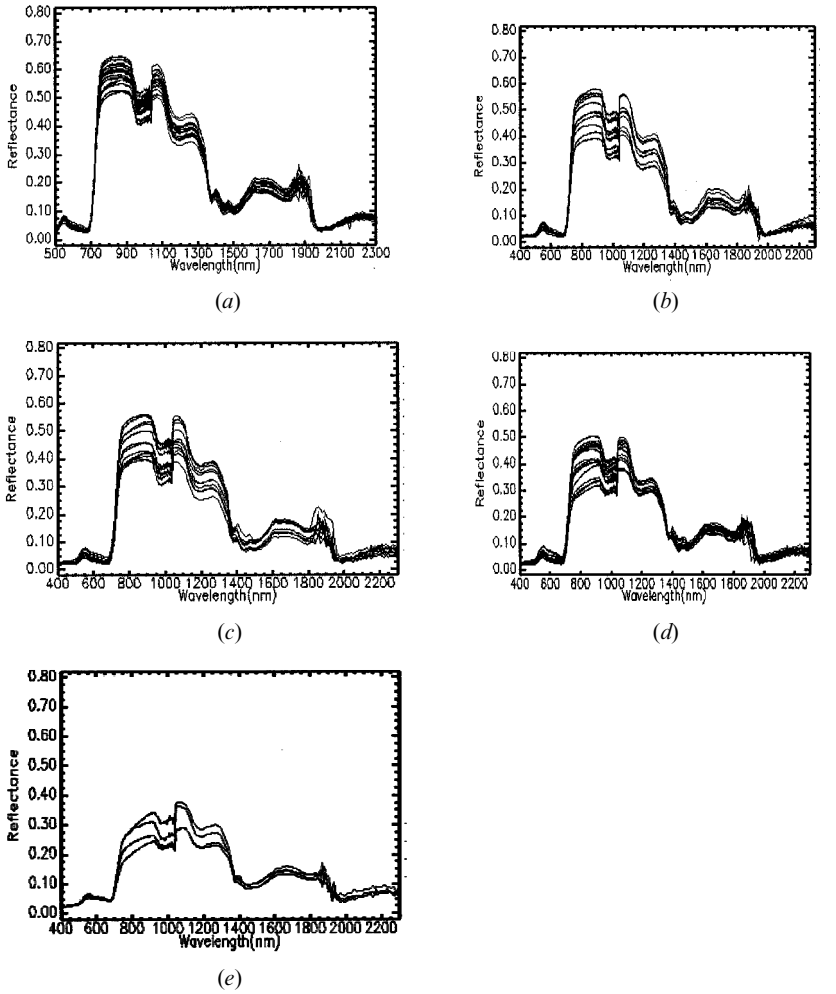


Figure 1. Spectra samples of (*a*) healthy tomatoes, (*b*) late blight infection stage 1, (*c*) late blight infection stage 2, (*d*) late blight infection stage 3, (*e*) late blight infection stage 4.



variable, we ran PCA on the 66 spectra for the identification of the principal components, which were expected to be able to discriminate the healthy tomato plants from the diseased ones.

2.2.3. *Cluster analysis*

Cluster analysis is the generic name for a multivariate procedure of clumping similar objects into categories, enabling identification of the basic structure in the data set. No training or prior knowledge of data distribution is required for the analysis. Therefore, clustering can be a subjective, exploratory procedure. Despite the obvious benefits of cluster analysis with respect to identifying structures, there are two related concerns in this method: (1) determining the number of clusters and (2) deciding whether a solution is significant (Holden and LeDrew 1998). However, in addition to pre-knowledge and intuition about the subject, no other methods can be applied statistically to determine or select the number of clusters or methods. For

our analysis, we selected the Centroid method based on the squared Euclidean distance as the condition for grouping samples into clusters.

2.2.4. *Spectral ratio analysis*

Following the question of spectral discrimination, there is an additional question in applying remote sensing to detect plant stresses: what are the wavelengths that are sensitive to plant stresses caused by late blight infection? We assumed that soil has approximately the same impact on each spectral measurement in the field. Our data set of this study indicated the minimal influence of soils on canopy spectra. We can therefore expect that by calculating spectral ratios, the impact of soil on spectral measurements can be removed or reduced to a minimum. Wavelength sensitivity analysis would then be improved. Because our objective was to investigate discrimination between spectra of healthy and late blight infected plants, we used the spectra of healthy plants as the denominator when calculating ratio spectra. If any two spectra are similar over the entire spectrum wavelength, we expect to have a ratio value around 1, which means that the spectrum in the numerator also represents healthy tomato canopies. If any two spectra are different over the entire spectrum wavelength, we expect to have ratio values farther from 1, which means that the spectrum in the numerator would represent infected canopies. The more the ratio values deviate from 1.0, the severer the infections would be.

Therefore, taking the mean spectrum of healthy plants as the denominator, the ratio spectrum was calculated for each late blight infection stage with its mean spectrum as the numerator. The formula is:

$$\mathrm{SRatio} = \mathrm{LBMSP}/\mathrm{HMSP} \tag{1}$$

where SRatio is the spectral ratio, HMSP is the mean spectrum of healthy plants, and LBMSP is the mean spectrum of late blight infected plants. Figure 2 illustrates the mean spectra of healthy plants, and late blight infected plants with stages 1 to 4.

## 3. Results

3.1. *Principal component analysis*

PCA revealed that the first eigenvector accounted for 58.73% of the variance of the original data set and the second for 35.51%. All of the other eigenvectors only accounted for the remaining 5.76%. Therefore, the first two eigenvectors can be regarded as the principal components and the rest can be dropped from further analysis. The distribution of eigenvalues among the eigenvectors is illustrated in figure 3(a). PCA also showed that the first principal component had a high, positive linear correlation to the canopy spectra of healthy tomato plants, and the second principal component to the late blight infections in stage 3 and stage 4. The values of the two principal components are displayed in figure 3(b). The percentage of spectral samples with positive and negative linear correlation with the two principal components is given in table 2, which clearly shows that each principal component represents the amount of spectra samples under various infection stages. Based on this percentage, the discrimination ability of the principal components can be interpreted.

As the principal components are orthogonal to each other, and each spectral sample can be represented by the linear combination of these principal components, it can be seen that the entire set of spectral samples are dominated by these two principal components. Since the first principal component has positive correlation

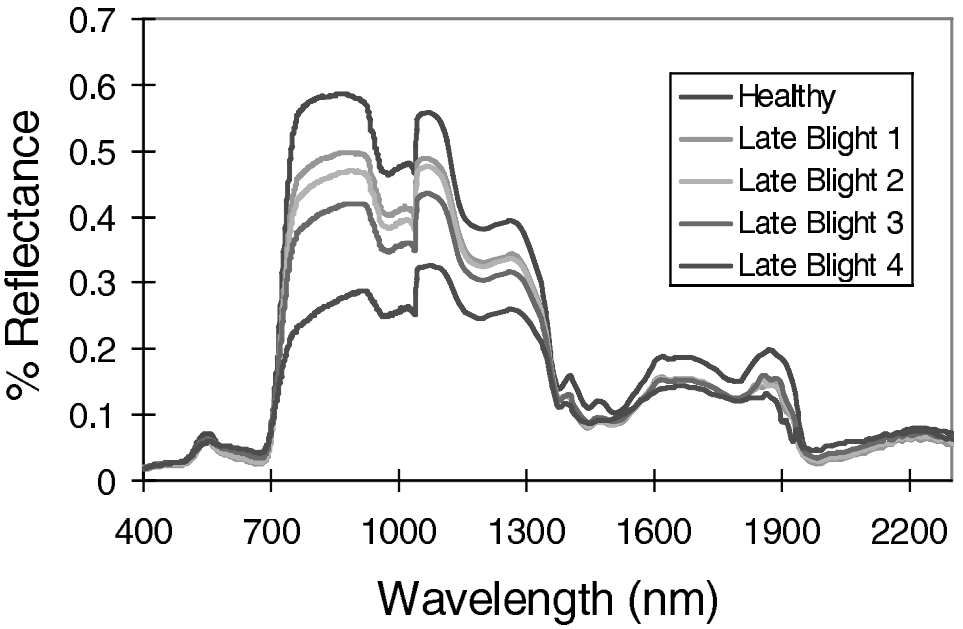


Figure 2. Mean spectra of the healthy and infected tomato plants at infection stages 1, 2, 3, and 4.

with 100% samples of healthy plants and negative correlation with 77% and 100% samples of infected plants at stages 3 and 4 respectively, we can interpret it as a representation of healthy plants. Similarly, the second principal component represents the severely infected plant samples due to its high percentage of samples having positive correlation with infection stages 3 and 4 and negative correction with healthy plants. Thus, we can conclude that healthy plants and late blight infected plants can be successfully discriminated using these two principal components. Table 2 also clearly indicates that more reliable discrimination can be obtained when the infected tomato plants are at infection stage 3 or above. It is more difficult to discriminate healthy tomato plants from infected tomato plants if the infection has only reached stages 1 or 2.

### 3.2. *Cluster analysis*

The cluster tree for classification is displayed in figure 4. Based on the cluster tree graph and the corresponding spectral samples, we performed statistics to establish the association between each cluster and each type of spectra. Table 3 gives the results of the statistics at three thresholds.

When the distance of 0.5 is used as the cut-off point, all the 66 spectra samples can be grouped into five clusters. The first cluster contains 76% of spectra samples with healthy tomato plants, 16% with the infected plants of stage 1 and 8% stage 2. Therefore, it can be said that this cluster is a representation of healthy tomato plants mixed with some light infection ones. Since the second cluster contains 14% of spectra samples with the healthy tomato plants, 24% with the infected plants of stage 1, 19% stage 2 and 43% stage 3, respectively, it can logically be said that it represents the infected plants of stage 3. The third cluster represents infected plants at stages 2 and 3 because it contains 18% of spectra samples with the infected plants

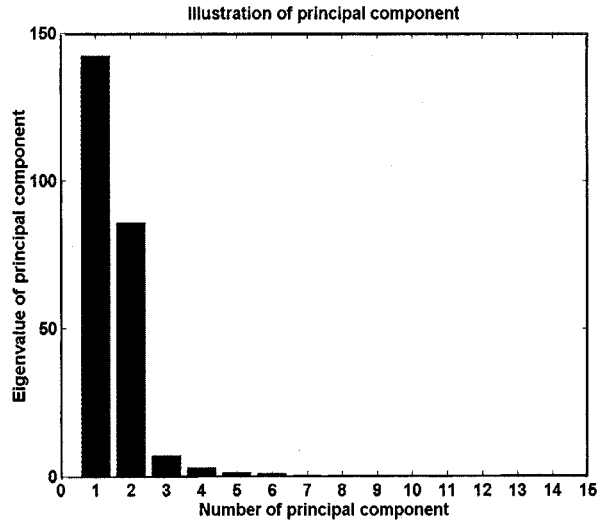


(*a*)

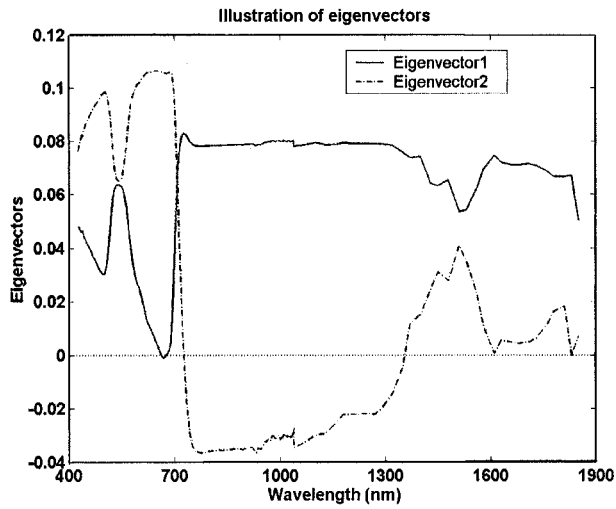


(*b*)

Figure 3. (a) Eigenvalues for each principal component. (b) The first and second eigenvectors, i.e., the first two principal components.

of stage 1, 41% stage 2 and 41% stage 3. The fourth cluster represents infected plants at stages 3 and 4 due to its high percentage of the two spectra samples (67% and 33% respectively). The fifth cluster is surely a representation of severe infection plants because it only contains the spectra samples of infection plants at stage 4.

If the threshold 0.75 is used, three clusters are found. The first cluster contains 76% of spectra samples with healthy tomato plants, 16% with the infected plants of stage one and 8% stage two. Thus it is mainly a cluster of healthy plants. The second cluster contains 9% of spectra samples with healthy tomato plants, 21% with the infected plants of stage 1, 27% stage 2 and 43% stage 3. Therefore, it mainly represents the moderate to severe infection plants. The third cluster is composed of

Table 2. Percentage of spectral samples with positive (P) and negative (N) linear correlation to the two principal components.

| Infection stages | First principal component (PC1) | Second principal component (PC2) |
|---|---|---|
| Healthy plants | P ~ 100% | P ~ 23% |
| Stage 0 | N ~ 0% | N ~ 77% |
| Late blight infection | P ~ 45% | P ~ 10% |
| Stage 1 | N ~ 55% | N ~ 90% |
| Late blight infection | P ~ 42% | P ~ 25% |
| Stage 2 | N ~ 58% | N ~ 75% |
| Late blight infection | P ~ 23% | P ~ 65% |
| Stage 3 | N ~ 77% | N ~ 35% |
| Late blight infection | P ~ 0% | P ~ 100% |
| Stage 4 | N ~ 100% | N ~ 0% |



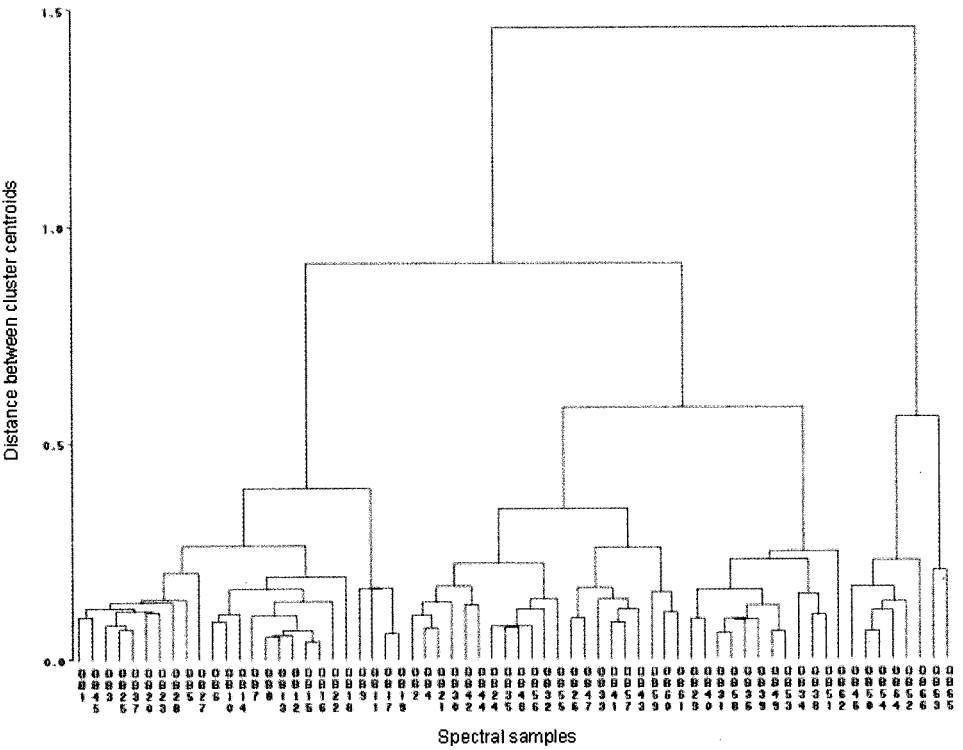


Figure 4. Cluster tree for classification of the spectral samples. OB 1–22 refer to the healthy tomato samples, OB 23–33 to late blight infection stage 1 samples, OB 34–45 to stage 2 samples, OB 46–62 to stage 3 samples, OB 63–66 to stage 4 samples.

two spectra samples with equal percentages of infected plants of stages 3 and 4. Thus, it represents the severe infection plants.

If we use the distance of 1 as threshold, only two clusters are found. The first cluster contains 38% of spectra samples with healthy tomatoes, 19% with the infected plants of stage 1, 19% stage 2, and 24% stage 3. Thus, it represents the healthy and light infection plants. However, the percentage of healthy plants is low. This makes

Table 3. Percentage of spectral samples for each cluster under different thresholds.

| Thresholds (Euclidean distance squared) | Cluster 1 | Cluster 2 | Cluster 3 | Cluster 4 | Cluster 5 |
|---|---|---|---|---|---|
| 0.5 | H—76%<br>LB1—16%<br>LB2—8% | H—14%<br>LB1—24%<br>LB2—19%<br>LB3—43% | LB1—18%<br>LB2—41%<br>LB3—41% | LB3—67%<br>LB4—33% | LB4—100% |
| 0.75 | H—76%<br>LB1—16%<br>LB2—8% | H—9%<br>LB1—21%<br>LB2—27%<br>LB3—43% | LB3—50%<br>LB4—50% | | |
| 1.0 | H—38%<br>LB1—19%<br>LB2—19%<br>LB3—24% | LB3—50%<br>LB4—50% | | | |

Note: H refers to healthy tomato plants. LB1, LB2, LB3, and LB4 to infected plants at infection stages 1, 2, 3, and 4 respectively.



it difficult to interpret. The second cluster contains 50% of spectra samples with the infected plants of stage 3 and 50% stage 4.

Based on the above analysis, it can be concluded that the classification with threshold of 0.75 is the best. Accordingly, three clusters are generated (table 3), which can provide the best discrimination of the samples with various infection stages. Since cluster 1 represents 76% spectra samples of healthy tomato plants, it should be interpreted as the representation of healthy plants. Similarly, cluster 2 represents infected plants at stage 3, and cluster 3 represents the infected plants at both stages 3 and 4.

Thus, our cluster analysis indicates that the healthy tomato plants can be spectrally separated from infected plants when late blight infection reaches stages 3 and 4. There is no cluster in which late blight stages 1 and 2 have dominant percentages. Thus, we can conclude that diseased plants at stages 1 and 2 are difficult to separate from healthy ones. This finding is consistent with that derived from PCA results.

### 3.3. *Spectral ratio analysis*

All the related spectral ratios are illustrated in figure 5. Large magnitude differences among spectral ratios can be observed for the wavelength range of 700–1300 nm. The results of ratio analysis showed the following wavelengths that are most sensitive to the degree of late blight infections on tomatoes and can be better utilized for discriminating healthy and late blight infected plants:

1. At the wavelengths around 543 nm, the first ratio valley (figure 5) observed in the range is possibly corresponding to the green peak
2. At the wavelengths around 663 nm, the first ratio peak (figure 5) next to the first valley is likely corresponding to chlorophyll absorption
3. At the wavelengths around 761 nm, the second ratio valley (figure 5) is probably corresponding to the 'red' edge
4. At the wavelengths around 1993 nm, the last peak (figure 5) is probably corresponding to the water absorption

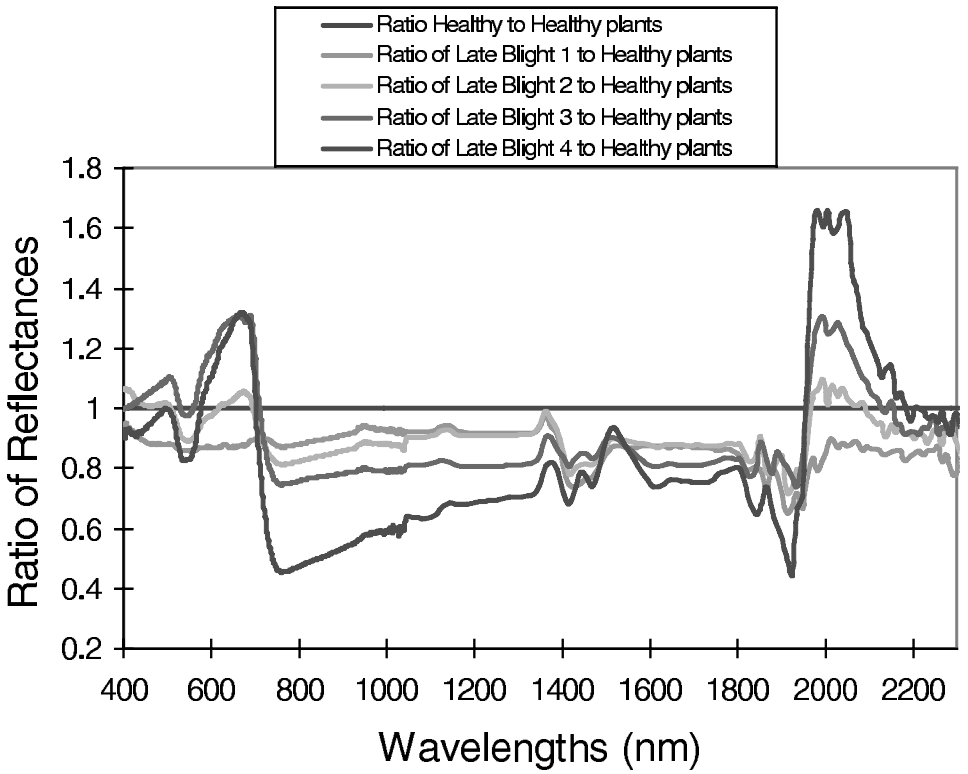


Figure 5. Mean ratio spectra of the infected samples with healthy spectrum as denominator.

Spectral differences among various infection stages are greater in these wavelengths. In other words, these wavelengths are more sensitive than others in terms of late blight infection detection through remote sensing. During the pathogen penetration and germination process, tomato plants react to the stimulation and infection of the disease by producing different levels of chlorophyll and other pigment concentrations. The change of these biochemistries on the plants leads to the differences in light responses of plant canopies, hence, the different reflectance resulted from the canopies with various infections. This distinct feature can then be utilized for discrimination of late blight infected tomato plants from the healthy ones and discrimination of late blight infection stages among the infected plants.

## 4. Discussion

Remote sensing technology offers a unique tool for monitoring disease development along with weather conditions (Lillesand and Kiefer 1994). The separation of the spectra of healthy tomato plants from infected ones with infection stage 3 or above is reliable due to the consistency of the results from both PCA and cluster analysis. Similar successful examples have been found by Holden and LeDrew (1998) who used spectral properties to discriminate healthy and unhealthy corals. Much work has been done to identify spectral properties for agricultural crops (Daughtry and Walthall 1998) and the infected crops of barley and beans (Lorenzen and Jensen 1989, Malthus and Madeira 1993). Blazquez and Edwards (1983) reported spectral reflectance of tomato and potato diseases under the controlled environment. They

concluded that the greatest changes in reflectance were detected in the chlorophyll absorption and near infrared regions of the spectrum, which is consistent with what we observed in our results for the degrees of late blight infection on tomatoes. Although some laboratory work has been done in characterizing the spectral properties for tomato, potato, beans and barley diseases (Blazquez and Edwards 1983, Lorenzen and Jensen 1989, Malthus and Madeira 1993), we first reported the successfulness of discriminating the spectra of healthy tomato plants from the infected ones under the field conditions.

This work provides a better understanding of the spectral properties of late blight infection on tomatoes and their light responses on tomato canopies. The identified wavelengths in the green region and near infrared region that are sensitive to the change of chlorophyll content and water content in the ratio analysis are consistent with previous work documented by Gitelson and Merzlyak (1997, 1998). The infected plants often contain lower chlorophyll levels that leads to a low photosynthesis rate and lower water content. The changes of these pigments and water content are often indicators of plant stress, which can be used to monitor the conditions of crop growth and site characteristics.

Though we are able to spectrally discriminate healthy tomatoes from infected tomatoes, we also understand the difficulties due to the similarity among vegetation spectra and other environmental influences. In this study, soil spectra were similar from field to field and the canopy was at full or close to full canopy closure when the spectra samples were collected. This provides a premise that our analysis would not be significantly influenced by soil background. However, the influence of soil background should be taken into consideration in the spectral analysis where large variability of soils exists and crop growth is largely affected by the environmental conditions. Sample size can be another important factor in deriving the conclusions. In this study, though there were some differences among spectra for the healthy tomato plants and infected ones with stages 1 and 2, they were not statistically significant enough to lead to a bias in the results of PCA and cluster analysis. We suspect that the small spectra sample size (Ahlbom 1993) for the infected tomato plants with stages 1 and 2 may be a factor for not being able to separate the infected plants at early infection stages, namely stages 1 and 2. If we could obtain more field spectra with late blight infection stages 1 and 2, we believe that the larger sample size will increase the statistical power to better discriminate the infected tomatoes at the early stage from healthy ones. However, without verification from larger sample size spectra for these early infection stages, the current observed spectral differences for the plants of infection stages 1 and 2 from healthy tomatoes could be due to random errors. We cannot statistically draw a conclusion that the spectra of the infected plants at stages 1 and 2 are significantly different from the spectra of healthy plants. Therefore, further research is needed with larger samples of the early infection stages in order to be certain that the infection at stages 1 and 2 can also be discriminated from healthy plants.

Nonetheless, the infection at stage 3 or above can be successfully discriminated from healthy plants. In fact, around infection stage 3, some of the spots in the field(s) are already severely infected by late blight, and at this stage economic losses start to occur. The developed relationships between the late blight infection on tomatoes and their spectral properties identified in this study could enable us to use the extracted information as a training set to classify the remotely sensed images for disease detection. The synoptic view and the repetitive cover afforded by satellite

data allow multi-temporal observation of seasonal changes. If farmers have access to the classified disease map for their fields of tomatoes, they would be in a better position for monitoring/controlling late blight infection in their fields. Farmers could then order pesticide applications accordingly to protect their crop productions.

It is known that late blight survives on volunteer plants and on abandoned plant materials. Sporangia serve as the primary inoculums and are carried by wind to other plants (Agrios 1997). Applying protective pesticides at that time cannot cure the infected canopies in the infected spots, but it can prevent the spread of the disease to other locations within the field or to other fields. Hence, farmers can control the disease in the infected areas and protect the areas that are not affected, to increase the productivity and the quality of the tomato fruits. In this way, farmers can have a direct understanding of the field conditions and the exact location and extent of the infection. Farmers can precisely and economically apply pesticides to the specific infected area. This technology can help farmers to increase the productivity of tomatoes and minimize the environmental impacts by precisely applying pesticides both spatially and temporally. However, to make best use of such information, it is necessary to combine it with other data. The need for a marriage between remote sensing and ground truth, spatial and statistical analysis techniques is readily apparent and is made manifest through the adoption of Geographic Information System (GIS) and databases within all crop assessment methodologies. These systems and methodologies represent an essential tool for the enhancement of traditional disease management techniques. This research provided a first step in best utilizing the developed technologies for precision disease management in sustainable agriculture.



## 5. Conclusions

Using remotely sensed canopy reflectance data, healthy tomato plants can be successfully discriminated from the plants of late blight infection when the infection reaches stage 3 or above. The spectral bands of green to red and near infrared are associated with the important spectral features of late blight infection on tomato plants. These wavelength regions include the green peak wavelengths at around 543 nm, chlorophyll absorption wavelengths at around 663 nm, the 'red edge' wavelengths at around 761 nm, near infrared wavelengths 761–1300 nm, and water absorption wavelengths at around 1993 nm.

The results indicated that remote sensing could be used to identify, and possibly diagnose, infections of tomato canopies. By understanding the spectral response of economically important diseases, we can use the technology to provide farmers with information to better protect their crops and reduce farming costs. From an environmental viewpoint, such information will help reduce environmental pollutions from pesticide applications by more accurately and precisely applying pesticides to crop fields. In the coming decades, agriculture will no doubt take advantage of the available technologies in farm management. This research lays a foundation for precise disease management once high-resolution remote sensing systems are commercially available.

**Acknowledgments**

We wish to acknowledge Carla Thomas for guiding the field identification of the disease, Monica Garcia for assisting the field data collection. We thank Erin Anderson and Dr. Shawn Smallwood for comments on the earlier draft of this manuscript. We also wish to thank Zeneca Ag Products for partial financial support for this research.

## References


AGRIOS, G. N., 1997, *Plant pathology* (San Diego: Academic Press).

AHLBOM, A., 1993, *Biostatistics for epidemiologists* (Boca Raton: Lewis Publishers).

BLAZQUEZ, C. H., and EDWARDS, G. J., 1983, Infrared color photography and spectral reflectance of tomato and potato diseases. *Journal of Applied Photographic Engineering*, **9**, 33–37.

BOWMAN, A. P., WINTER, E. M., STOCKER, A. D., and LUCEY, P. G., 1999, Hyperspectral infrared techniques for buried landmine detection. *Proceedings of the Fourth International Airborne Remote Sensing Conference and Exibition/21st Canadian Symposium on Remote Sensing, Ottawa, Canada, 21–24 June 1999* (Ann Arbor, MI: ERIM International Inc.), pp. 19–26.

BRYANT, R. B., and MORAN, M. S., 1999, Determining crop water stress from crop temperature variability. *Proceedings of the Fourth International Airborne Remote Sensing Conference and Exibition/21st Canadian Symposium on Remote Sensing, Ottawa, Canada, 21–24 June 1999* (Ann Arbor, MI: ERIM International Inc.), pp. 289–296.

DAUGHTRY, C. S. T., and WALTHALL, C. L., 1998, Spectral discrimination of *Cannabis sativa* L. leaves and canopies. *Remote Sensing of Environment*, **64**, 192–201.

DEGUISE, J. C., MCNAIRN, H., STAENZ, K., and MCGOVERN, M., 1998, Spatial high resolution crop measurements with airborne hyperspectral remote sensing. *Proceedings of the Fourth International Conference on Precision Agriculture and Other Precision Resources Management, St. Paul, Minnesota, 18–22 July 1998* (Ann Arbor, MI: ERIM International Inc.), pp. 1603–1608.

DEGUISE, J. C., and STAENZ, K., 1999, Agricultural applications of airborne hyperspectral data: weed detection. *Proceedings of the Fourth International Airborne Remote Sensing Conference and Exibition/21st Canadian Symposium on Remote Sensing, Ottawa, Canada, 21–24 June 1999* (Ann Arbor, MI: ERIM International Inc.), pp. 352–358.

DUNTEMAN, G., 1984, *Introduction to Multivariate Analysis* (Newbury Park, CA: Sage).

FUNG, T., and LEDREW, E., 1987, Application of principal component analysis to change detection. *Photogrammetry Engineering and Remote Sensing*, **53,** 1649–1658.

GITELSON, A. A., and MERZYLAK, M. N., 1997, Remote estimation of chlorophyll content in higher plant leaves. *International Journal of Remote Sensing*, **18**, 2691–2697.

GITELSON, A. A., and MERZYLAK, M. N., 1998, Remote sensing of chlorophyll concentration in higher plant leaves. *Advanced Space Research*, **22**, 689–692.

HOLDEN, H., KALBFLEISCH, W., NEWMAN, C., and LEDREW, E., 1999, Hyperspectral identification of coral reef features. *Proceedings of the Fourth International Airborne Remote Sensing Conference and Exibition/21st Canadian Symposium on Remote Sensing, Ottawa, Canada, 21–24 June 1999* (Ann Arbor, MI: ERIM International Inc.), pp. 129–135.

HOLDEN, H., and LEDREW, E., 1998, Spectral discrimination of healthy and non-healthy corals based on cluster analysis, principal components analysis and derivative spectroscopy. *Remote Sensing of Environment*, **65**, 217–224.

LEBLANC, S. G., CHEN, J. M., MILLER, R. J., and FREEMANTLE, J., 1999, Compact Airborne Spectrographic Imager (CASI) used for mapping LAI of cropland. *Proceedings of the Fourth International Airborne Remote Sensing Conference and Exibition/21st Canadian Symposium on Remote Sensing, Ottawa, Canada, 21–24 June 1999* (Ann Arbor, MI: ERIM International Inc.), pp. 297–303.

LILESAND, T. M., and KIEFER, R. W., 1994, *Remote Sensing and Image Interpretation*, 3rd edn (New York: John Wiley & Sons).

LORENZEN, B., and JENSEN, A., 1989, Changes in leaf spectral properties induced in barley by cereal powdery mildew. *Remote Sensing of Environment*, **27**, 201–209.

MALTHUS, T. J., and MADEIRA, A. C., 1993, High resolution spectroradiometry: Spectral reflectance of field bean leaves infected by *Botrytis fabae*. *Remote Sensing of Environment*, **45**, 107–116.

WINTER, E. M., and SCHLANGEN, J. M., 1999, Comparison of techniques for the classification of vegetation using a hyperspectral sensor. *Proceedings of the Fourth International Airborne Remote Sensing Conference and Exibition/21st Canadian Symposium on Remote Sensing, Ottawa, Canada, 21–24 June 1999 (Ann Arbor, MI: ERIM International Inc.),* pp. 723–728.